Electrical Power and Energy Systems 69 (2015) 273–286

Contents lists available at ScienceDirect

Electrical Power and Energy Systems

journal homepage: www.elsevier.com/locate/ijepes

Stochastic frequency-security constrained energy and reserve management of an inverter interfaced islanded microgrid considering demand response programs

Navid Rezaei, Mohsen Kalantar *

Center of Excellence for Power Systems Automation and Operation, Electrical Engineering Department, Iran University of Science and Technology (IUST), Tehran, Iran

ARTICLE INFO

Article history:
Received 14 July 2014
Received in revised form 1 December 2014
Accepted 14 January 2015

Keywords:
Microgrid
Hierarchical frequency control
Energy management system
Demand response
Stochastic programming

ABSTRACT

This paper addresses a novel security constrained energy management system of a microgrid which considers the steady-state frequency. Microgrid frequency as a key control variable, continuously exposes to be excursed of its nominal value due to unpredictable intermittencies arise from renewable sources and/or load consumptions. Moreover, great utilization of inertia-less inverter-interfaced distributed energy resources intensifies potential frequency excursions. As a result, energy and reserve resources of a microgrid should be managed such that the microgrid frequency lies within secure margins. To that end, a new objective function on the basis of the frequency dependent behavior of droop-controlled distributed generations is formulated using a mixed integer linear programming. It is aimed to optimize the microgrid frequency according to the economic and environmental policies. Besides, to seek the active participation of the consumers into proposed frequency management approach, a linearized ancillary service demand response program is also proposed. In addition, to properly model the impacts of microgrid various uncertainties in the frequency management approach, a two-stage stochastic optimization algorithm is employed. Simulations are performed in a typical microgrid which operates in the islanded mode during a 24 h scheduling time horizon. The numerical results show the impressiveness of the proposed frequency aware energy management system while concurrently managing the microgrid security and economical aspects. Furthermore, it is demonstrated that utilization of demand response programs economizes the microgrid frequency management approach.

Introduction

Recently, microgrid idea has been introduced to transform the conventional power systems to a more reliable, carbonless and economical system. To that end, microgrids exploit efficient energy management systems (EMS) to ensure from a robust and efficient operational planning. Generally, EMS is in charge to provide a proper synchronization with the main grid, optimal frequency and voltage control and improvement the required reliability and security margins of the microgrid [1–5].

The microgrids are continuously encountered to the power fluctuations stem from intermittent renewable energy sources (RESs), load demand variations and possible line/unit contingencies. This puts the microgrid frequency security at risk of instability [4]. Meanwhile, due to the higher ratio of the power variations to the small scale energy capacity of the islanded microgrids, the importance of frequency management will be doubly critical. Moreover, considering to the characteristics of the produced energy, Distributed Energy Resources (DERs) are usually operated via the inertia-less static voltage source inverters (VSIs) as interfaces between the microgrid and the DER technologies [6]. Consequently, this intensifies the frequency security importance and necessitates more attendance with respect to the microgrid frequency control issues. To control the microgrid frequency reliably, different energy and reserve resources should be coordinately managed regarding to the cost-emission policies of the microgrid energy management system. By this way, both the security and economical goals of the microgrid will be achieved.

The frequency security preservation of the microgrids operating in the islanded mode is more crucial. Therefore, the EMS should adopt a reliable control strategy to properly manage the DERs outputs with a reasonable operation cost and emission. One of the promising frequency control methodologies usually used in the

* Corresponding author at: Narmak, Tehran 1684613114, Iran. Tel.: +98 2173225662; fax: +98 2173225662.
E-mail addresses: nrezaei@iust.ac.ir (N. Rezaei), kalantar@iust.ac.ir (M. Kalantar).

http://dx.doi.org/10.1016/j.ijepes.2015.01.023
0142-0615/

Nomenclature

Indices

i	index of dispatchable distributed generation units (IIDGs) from 1 to Ng
k	index of demand response provider (DRP) from 1 to Nk
w	index of wind turbines from 1 to Nw
v	index of photovoltaic panels from 1 to Nv
s	index of scenarios from 1 to Ns
h	index of hours from 1 to Ns
l	index of frequency control level could be equal to *pri* (primary) and *sec* (secondary)
ud	index of scheduled reserves could be *up* or *down*

Parameters and constants

$m_p(i)$	frequency droop parameter of IIDG i
f_{ref}	microgrid reference frequency
Δf_l^{max}	maximum allowable microgrid frequency excursion limit during control level l
a_i	fixed operation cost of IIDG i
b_i	first-order operation cost of IIDG i
C_i^{SU}	start-up cost of IIDG i
C_i^{SD}	shut-down cost of IIDG i
$\rho_i(l,ud)$	cost up/down reserve of IIDG i in control level l
ρ_w	cost of operation of wind turbine w
ρ_v	cost of operation of photovoltaic panel v
$P_g^{max}(i)$	upper level of active power generation of IIDG i
$P_g^{min}(i)$	lower level of active power generation of IIDG i
$ramp_i^{up}$	ramp-up limit of IIDG i
$ramp_i^{dn}$	ramp-down limit of IIDG i
$ramp_i^{su}$	start-up ramp of IIDG i
$ramp_i^{sd}$	shut-down ramp of IIDG i
$\Omega_i^{CO_2}$	CO_2 emission rate of IIDG i
$VOLL$	value of lost load
$Load(h)$	forecasted load consumption at hour h
$P_w(w,h)$	forecasted active power output of wind turbine w at hour h
$P_v(v,h)$	forecasted active power output of photovoltaic panel v at hour h
$\rho_d^R(k)$	reserve cost of DRP k
$\alpha_m(k)$	cost of block m in DRP k offer package

Variables

π_s	probability of scenario s
$\Delta f(s,l,h)$	microgrid frequency deviation in scenario s, control level l and at hour h
$\Delta P_g(s,i,l,h)$	active power deviation of IIDG i in scenario s, control level l and hour h
$\Delta Pd(s,k,l,h)$	accepted load reduction of DRP k in scenario s, control level l and hour h
$\Delta P_w(s,w,l,h)$	active power deviation of wind turbine w in scenario s, control level l and hour h
$\Delta P_v(s,v,m,h)$	active power deviation of photovoltaic panel v in scenario s, control level m and hour h
$\Delta P_{ref}(s,i,l,h)$	reference power deviation of IIDG i in scenario s, control level l and hour h
$\Delta Load(s,l,h)$	active power deviation of microgrid load in scenario s, control level l and hour h
$Pd_m(k,h)$	demand of block m in DRP k offer package in hour h
$W_{i,h,s}^{IIDG}$	binary variable indicating availability status of IIDG i in scenario s and hour h
$Pd(k,h)$	load reduction of DRP k at hour h
$P_g(i,h)$	active power output of IIDG i at hour h
$D(s,l,h)$	frequency elasticity of microgrid loads in scenario s, control level l and hour h
$P_{ref}(i,h)$	reference power set point of IIDG i at hour h
$R_g(i,l,ud,h)$	scheduled up/down reserve of IIDG i in control level l and hour h
$R_d(k,l,ud,h)$	scheduled up/down reserve of DRP k in control level l and hour h
$P_g^s(i,l,h)$	active power output of IIDG i in scenario s, control level l and hour h
$Pd^s(k,l,h)$	load reduction of DRP k in scenario s, control level l and hour h
$P_{ref}^s(i,l,h)$	reference power of IIDG i in scenario s, control level l and hour h
$P_w^s(w,l,h)$	active power output of wind turbine w in scenario s, control level l and hour h
$P_v^s(v,l,h)$	active power output of photovoltaic panel v in scenario s, control level l and hour h
$LSH(s,l,h)$	load to be shed unwillingly in scenario s, control level l and hour h
$u(i,h)$	binary variable indicating commitment state of IIDG i at hour h
$y(i,h)$	binary variable indicating start-up state of IIDG i at hour h
$z(i,h)$	binary variable indicating shut-down state of IIDG i at hour h
$u^l(i,h)$	binary variable indicating commitment state of IIDG i at hour h and control level l

islanded microgrids is based on the P–f droop methods [6–8]. Indeed, droop based controllers behave as the mimics of the synchronous generator governors in which the power system frequency is controlled by adjusting the active power outputs of the committed generators [9–12]. Hence, by employing the P–f droop control scheme in Inverter Interfaced Distributed Generators (IIDGs), the microgrid frequency will suitably be controlled.

On the other hand, the participation of the IIDGs in the microgrid frequency control can be effectively managed through a hierarchical control structure. The hierarchical structure consists of Microgrid Central Controller (MGCC) as the main manager of the microgrid and some Local Controllers (LCs) which work based on the droop control method [13–16]. Inspired by traditional power systems, the control functions of LCs and MGCC can be classified as primary and secondary hierarchical frequency control levels, respectively [6,7,14,15]. Concisely, in the primary control level, droop controlled IIDGs immediately react to the frequency deviations by releasing the scheduled primary reserves. In the secondary control level, restoration and readjustment of the microgrid frequency are tackled by means of MGCC which can be accomplished subject to the operational policies of the EMS [17–19].

Recently, in the light of Demand Response (DR) concept driven by the smart grid initiative, consumers have also the chance to actively participate in the operational planning of the power systems. The consumer participation can be performed directly or by means of third utilities known as Demand Response Providers (DRPs). Owing to the DR definition [20,21], the consumers can take part in the energy management system, especially when the microgrid reliability is in question. Thus, the EMS can benefit from the capability of the DR programs in provision the frequency

control ancillary services and economizing the security management of the microgrid. For example, in [22] a full linear ancillary service demand response model has been proposed to incorporate the demand response resources in the energy and reserve scheduling of the large scale power systems. Also, the authors in [23–25] has presented a similar step-wise incentive-based demand response model to cope with the system uncertainties in the operational planning of the smart distribution power systems. In [26] the proposed DR response programs have been implemented by intermediary of a DRP. Indeed, DRP as an active aggregator is in charge to enable the participation of small consumers in the day-ahead energy and reserve scheduling by delegation between the DSO and end-user small consumers who assigned in the DR programs.

On the other hand, despite several researches have investigated different aspects of the microgrid energy management system, to the best of our knowledge, no work has been dedicated to study microgrid energy management considering to both security and economical objectives, particularly with the emphasis on the frequency control issues. In [27–30], a heuristic based multi-objective optimization approach has been employed to schedule the DERs in a microgrid. Also, in [31,32] energy management problem of an islanded MG has been carried out in order to maximize the utilization of the DERs with a cheap day-ahead operational cost. However, in the above mentioned references, the great impacts of suddenly load fluctuations or randomly RES power output variations on the microgrid resource scheduling were disregarded. Also, no attention paid to the procurement of the microgrid reserve requirements. In [33,34], using a stochastic-based optimization, day-ahead energy and reserve resources of a microgrid have been managed, however, the frequency dependent behavior of the DERs and its impact on the microgrid reserve scheduling has not been developed. Besides, in references [35–37], frequency based dynamic performance of the DERs has been modeled appropriately, however, precise reserve scheduling has been neglected and the optimization procedure performed over a few minute time horizon and did not cover the day-ahead energy requirements. Moreover, the great impacts of the RES unit uncertainties like wind turbines (WTs) or photovoltaic (PVs) were not considered. Likewise, though in admired work [38], the primary and secondary frequency control loops have been modeled appropriately, corresponding uncertainty resources were not modeled and the microgrid security requirements were not reported. By reviewing the literature, the lacuna of a detailed and thorough study on a frequency security constrained energy management system of the microgrids is still evident. Though precise scheduling and deployment of the primary and secondary reserve resources considering to the microgrid frequency management has been presented in [39], however, the productive role of the demand response programs has been neglected.

Worth mentioning that direct coupling to the system frequency, make the primary control reserves play as impressive variables in the microgrid energy management strategy. In order to fill this gap out, the steady-state frequency control performance of the VSIs are modeled precisely. On the basis of the derived modeling a new objective function which considers the microgrid day-ahead frequency profile is proposed in order to properly control the microgrid expected frequency excursions in a cost-effective scheme. By this way, both the economical and security-based purposes of the microgrid will be achieved. Furthermore, to promote the proposed EMS, a scenario-based two-stage stochastic programming is used to model the effects of the microgrid various uncertainties on the energy and reserve management problem. Furthermore, an ancillary service demand response program is modeled perfectly and managed in coordination with the IIDGs to cost-effectively control the microgrid frequency. The proposed energy management system solves a frequency-security constrained unit commitment problem of an islanded microgrid in a 24 h scheduling time horizon. The whole problem is modeled using the mixed-integer linear programming (MILP) to guaranty the optimality of the solution. In summary, the main contributions of the paper can be highlighted as:

- Precise modeling of the steady-state hierarchical frequency control functions of a droop controlled microgrid;
- Proposing a novel frequency dependent objective function to optimize the microgrid security;
- Integration an ancillary service demand response program into the proposed frequency management problem to ensure the microgrid frequency aware operational planning;
- Precisely scheduling of the microgrid day-ahead energy, primary and secondary control reserves through a well-organized stochastic MILP framework.

The remainder of the paper is organized as follows. In Section 'Hierarchical frequency control structure of microgrids', microgrid hierarchical energy management structure is briefly reviewed. Section 'Demand Response program' presents the proposed demand response program. In Section 'Model description and problem formulation' the mathematical model of the proposed two-stage stochastic MILP frequency control optimization is formulated. In Section 'Simulation and Numerical Results', simulation procedure in a microgrid test system is operated over a 24-h time horizon. The scheduled day-ahead energy and reserve resources are illustrated. Also, in this section, numerical results are analyzed. Lastly, some concluding remarks are presented in Section 'Conclusions'.

Hierarchical frequency control structure of microgrids

The hierarchical control structure of a microgrid including several DERs is illustrated in Fig. 1. In this scheme, it is assumed that all the dispatchable IIDGs are locally controlled by the P–f droop method. The IIDGs will be enabled to control the frequency excursions in proportion to their active power outputs [40]. Noteworthy, the RES units are not participated into the frequency control function and it is assumed that they generate the stochastic active power according around the forecasted values.

As depicted in Fig. 1, the droop controlled IIDGs automatically release the primary control reserves to compensate the microgrid frequency excursions. During this control level, not only the frequency will be controlled but also the energy demands are shared properly corresponding to the power ratings of the committed DERs. However, after the primary response of the droop controllers is fulfilled, the steady-state frequency may deviate from its nominal value due to the droop control inherent errors [5–7,40]. Therefore, the secondary control level as the highest level in an islanded microgrid will be activated. In this control level, the MGCC tries to compensate the frequency errors by bringing the steady-state frequency to a more secure range or even restoring the frequency to its rated value. Modification of the frequency in the secondary level can be obtained by readjusting the reference active power set-points of the dispatchable IIDGs. Noticeably, the active power set-points of the dispatchable IIDGs should be managed with respect to the EMS operational policies.

To describe the frequency dependent control functions of a droop controlled IIDG, the block-diagram of the hierarchical frequency control structure of an IIDG is illustrated in Fig. 2. Once an active power deviation ΔP_g is occurred in the microgrid, it is measured and calculated using Voltage and Current (V & I) measurement, active power calculation and Low-Pass Filter (LPF) units, respectively. The droop controller automatically changes the VSI produced frequency in proportion to the ΔP_g as expressed in

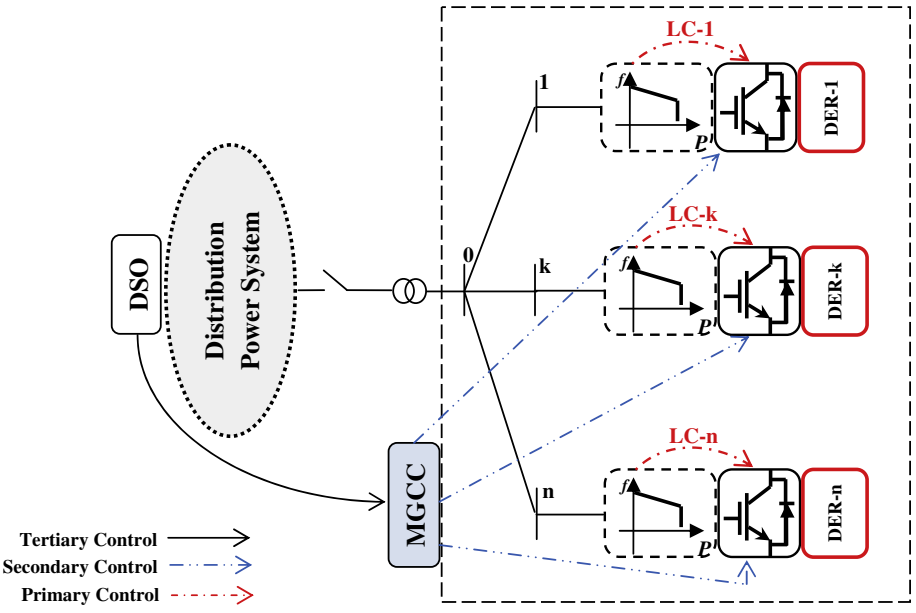

Fig. 1. Hierarchical frequency control structure of a droop-controlled microgrid.

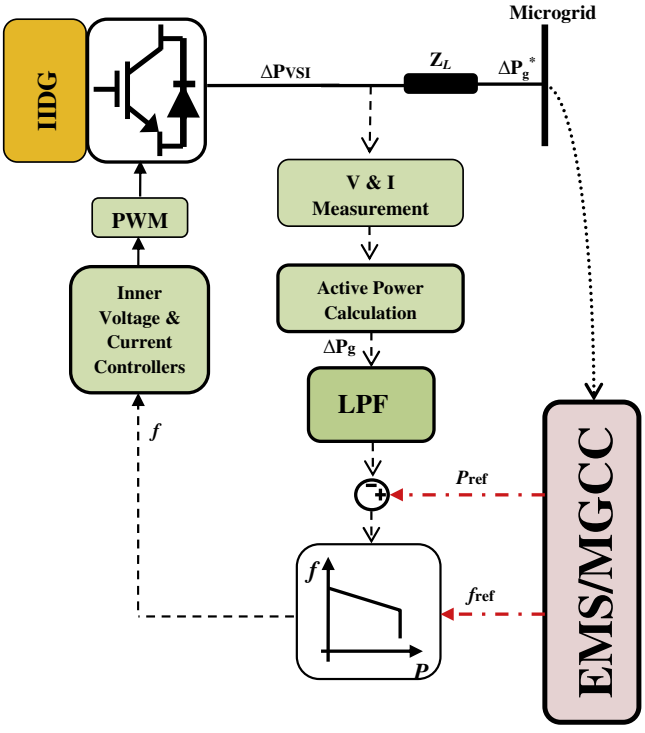

Fig. 2. Hierarchical frequency control levels of a droop-regulated IIDG.

Eq. (1). This control action is performed during the primary control level.

$$\frac{-1}{m_p}(f - f_{ref}) = \Delta P_g \tag{1}$$

The amount of the released primary reserve in the primary control level relies to the droop coefficient of the LC i.e. m_p and also the available capacity of the IIDG. The adjusted frequency is used by the VSI inner voltage and current controllers to generate the desired active power output (ΔP_{VSI}) by readjusting the PWM switching signals. The final compensating active power ΔP_g^* is injected to the microgrid after passing the impedance. It is assumed that the delay between primary source of the IIDG and the interfacing VSI is negligible and the DC link in the VSI is capable enough to supply the required power of the VSI. The adjusted primary frequency excursion may be out of the pre-specified secure ranges. In this case, the MGCC can restore the system frequency within the determined secure bounds by readjusting the reference active power set-points of the IIDGs, i.e. P_{ref}. The restoration process should be performed subject to the supervisory economical and environmental policies of the EMS. Noteworthy, the EMS module can be installed at the MGCC or be executed separately.

It should be mentioned there is an analogous control for the reactive power and the corresponding voltage deviations through Q–V droop method, which is not considered in this paper.

Besides, as it is observable in Fig. 1., in the grid-connected mode, to ensure an efficient sophisticated operational scheduling, the MGCC optimizes power exchanges with the main grid by properly coordination with the DSO. The interactions between the DSO and different MGCCs of several grid-connected microgrids can be also presented as the tertiary frequency control functions. In the tertiary control level, the DSO is in charge to operate the interconnected microgrids coherently subject to the up-stream power system policies. Moreover, the tertiary control level helps the MGCCs improving the associated control functions in accordance to the secondary level. In a nutshell, the hierarchical control and energy management system of a microgrid, through various power management strategies, not only should cost-effectively augment the reliability, sustainability and security levels, but also help improving power system restoration capability by provision adequate ancillary services.

Demand response program

Realizing the smart grid eventual targets cannot be provided without thoroughly paying attention to its substantial achievement, i.e. Demand Response (DR), which is concentrated on actively participation of the consumers in the power system operational planning. DR can help power system operators reducing the overall stresses in the terms of augmentation system reliability, particularly when it is expected to be in question. As mentioned,

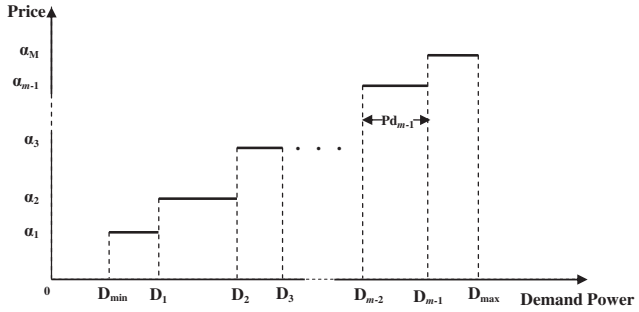

Fig. 3. Step-wise demand response price-demand curve.

frequency control in a microgrid is so crucial that acquires precise management of the energy and reserve resources. In this scheme, providing a coordinated contribution of the DR programs in the microgrid energy management system is a progressive step towards the microgrid eventual concepts. The EMS can exploit the DR advantages, specially the dispatchable incentive-based ones, to enhance the flexibility, efficiency and security indices of the microgrid. To the best of our knowledge, no attention has been paid to the usefulness of the DR programs in providing frequency control ancillary services in islanded microgrids. The present paper contributes to propose an ancillary service demand response program in the frequency management approach of a droop controlled islanded microgrid. It has been assumed that the proposed DR program can participate only in the secondary frequency control level of the hierarchical control structure. The reason is that in the secondary control level, there is enough time to reduce load consumptions properly, while in the primary level and without advanced control requirements, consumers may not be able to contribute in the frequency management procedure as fast as the droop controlled IIDGs are capable to. In this paper, it is assumed that consumers can participate in the microgrid energy management

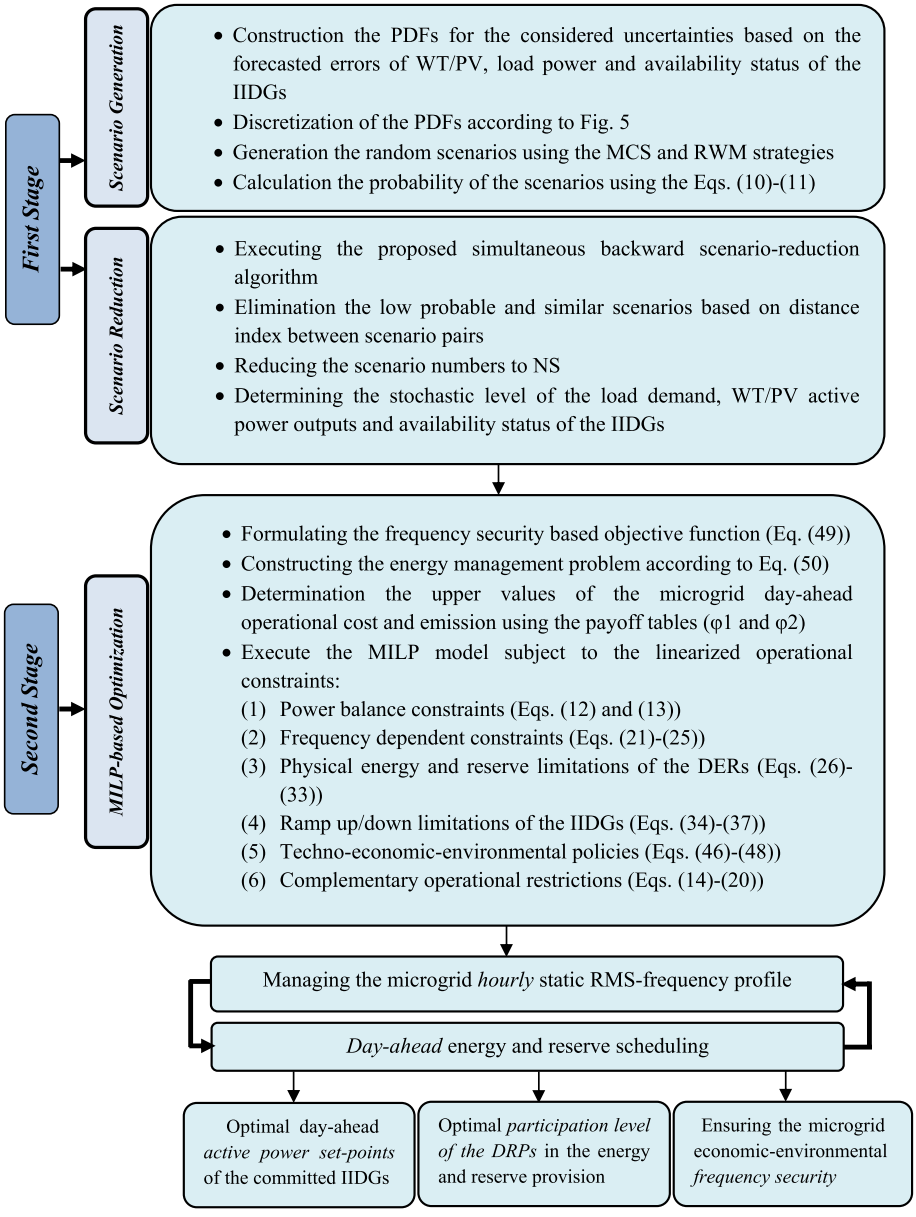

Fig. 4. Proposed two-stage stochastic MILP-based frequency management problem of microgrid.

system by intermediacy of a DRP. If it is needed, the DRPs are called by the EMS and paid in proportion to the performed load reductions. Each DRP submits its demand reduction bids in the form of a M step-wise price-demand package as depicted in Fig. 3.

D_{max} and D_{min} are sum of all deployed load curtailments and minimum acceptable load reduction that each DRP can carry it out, respectively. α_m and Pd_m are offered price and reduced demand level of mth step, respectively. Pd is total hourly curtailed load. R_d^{up} and R_d^{dn} are the scheduled up and down demand-side reserves, respectively which are presented by the DRP as the secondary control reserves. Eqs. (2)–(7) describing the proposed DR programs as follows:

$$D_{min} \leqslant Pd_m \leqslant D_m, \ \forall m = 1 \tag{2}$$

$$0 \leqslant Pd_m \leqslant D_m - D_{m-1}, \ \forall l = 2,3,\ldots,M \tag{3}$$

$$Pd = \sum_{m=1}^{M} Pd_m \tag{4}$$

$$D_{min} \leqslant Pd \leqslant D_{max} \tag{5}$$

$$Pd + R_d^{dn} \leqslant D_{max} \tag{6}$$

$$Pd - R_d^{up} \geqslant D_{min} \tag{7}$$

Costs associated to the participation of the consumers in the microgrid energy $\left(C_d^E\right)$ and reserve $\left(C_d^R\right)$ management are mentioned by Eqs. (8) and (9), respectively. c_d^{up} and c_d^{dn} are costs corresponding to the up and down scheduled demand response secondary control reserves, respectively.

$$C_d^E = \sum_{m=1}^{M} \alpha_m \cdot Pd_m \tag{8}$$

$$C_d^R = c_d^{up} \cdot R_d^{up} + c_d^{dn} \cdot R_d^{dn} \tag{9}$$

Model description and problem formulation

The MGCC is responsible for optimal reserve provision of the microgrids such that both the economical and security targets are achieved. The control functions of the MGCC are more crucial during the islanded operation where the various uncertainty resources have more dominant effects on the microgrid frequency and reserve management problem. In this paper, a well-organized two-stage MILP-based stochastic programming optimization is adopted to cope with the microgrid uncertainties. In the first stage, system uncertainties are modeled by generating some random scenario using Monte-Carlo Simulation (MCS) and Roulette Wheel Mechanism (RWM). Next, an efficient scenario reduction algorithm is employed to promote the computational effort of the model. In the second stage, the proposed frequency management approach is formulated using an MILP model. The optimization problem is solved according to the probabilities of the reduced scenarios. The general framework of the proposed two-stage stochastic optimization is presented in Fig. 4. Detailed descriptions are explained in the following.

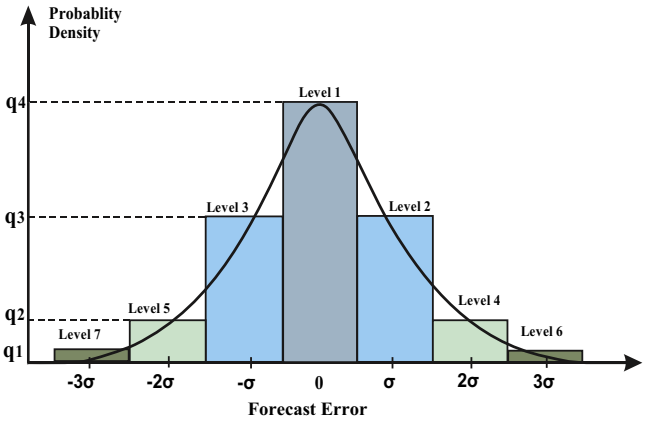

Fig. 5. Probability distribution function corresponding to the forecast errors.

First stage: Scenario generation and reduction

In order to model the uncertainties stem from the intermittent WT and PV power outages, load demands and the availability status of the IIDGs, the MCS and RWM strategies are employed to generate random scenarios with weighted probabilities. In this regard, first, the WT and PV forecast errors are modeled using normal Probability Distribution Functions (PDF) in which the mean values are equivalent to the forecasted values of the WT and PV output powers [41–43]. The load demand forecasted errors are also modeled in an analogous manner. In this paper, the assumed PDFs are divided into seven discrete intervals with different probability levels as illustrated in Fig. 5. Each interval has a width equal to σ which corresponds to the standard deviation of the WT/PV power outputs and load demand forecast errors. Then, the proposed RWM methodology is used to determine the stochastic level of the considered uncertainties. The forecast error probabilities are normalized and filled out over the range of between 0 and 1 as shown in Fig. 6. Then, using the MCS a random is generated in the range between 0 and 1. The normalized forecast error interval over the path in the roulette wheel in which the randomly generated number falls is selected as a scenario. It should be noted that the summation of normalized probabilities over the roulette wheel path are equal to one.

Moreover, to evaluate the robustness of the proposed frequency management procedure, an $N-1$ contingency analysis including IIDG random outages based on Forced Outage Rate (FOR) of the IIDGs is also simulated [43]. Similarly, a random number is generated in the range of $[0,1]$ using the MCS and compared to FOR of all the IIDGs. If the produced number is smaller than the FOR, the unit is out of service in that hour and scenario, otherwise, the IIDG is available. The final scenario is a vector consists of the produced scenarios for the WT/PV, load forecasted errors and the availability status of the IIDGs. Finally, the probability of each scenario is obtained by normalizing all the produced weighted scenarios as explained in Eqs. (10) and (11).

$$\pi_s = \frac{\prod_{h=1}^{Nh}\left(\left(\sum_{kl}^{7} W_{kl,h,s}^{L} \cdot q_{kl,h}\right) \cdot \left(\sum_{kw=1}^{7} W_{kwt,h,s}^{WT} \cdot q_{kwt,h}\right) \cdot \left(\sum_{kv=1}^{7} W_{kpv,h,s}^{PV} \cdot q_{kpv,h}\right) \cdot \left(\prod_{i=1}^{Ng} \gamma_{i,h,s}^{IIDG}\right)\right)}{\sum_{s=1}^{Ns}\prod_{h=1}^{Nh}\left(\left(\sum_{kl}^{7} W_{kl,h,s}^{L} \cdot q_{kl,h}\right) \cdot \left(\sum_{kw=1}^{7} W_{kwt,h,s}^{WT} \cdot q_{kwt,h}\right) \cdot \left(\sum_{kv=1}^{7} W_{kpv,h,s}^{PV} \cdot q_{kpv,h}\right) \cdot \left(\prod_{i=1}^{Ng} \gamma_{i,h,s}^{IIDG}\right)\right)}, \ \forall s = 1,\ldots,Ns \tag{10}$$

$$\gamma_{i,h,s}^{IIDG} = W_{i,h,s}^{IIDG} \cdot \left(1 - FOR_i^{IIDG}\right) + \left(1 - W_{i,h,s}^{IIDG}\right) \cdot FOR_i^{IIDG} \tag{11}$$

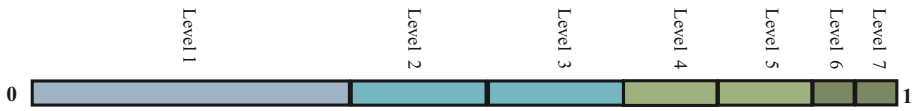

Fig. 6. Roulette Wheel Mechanism for normalized probabilities of considered forecast errors.

where $W^{L}_{kl,h,s}$, $W^{WT}_{kwt,h,s}$, $W^{PV}_{kpv,h,s}$ are binary variables indicating the status of selection of *kl*th load interval, *kwt*th wind turbine power interval, *kpv*th photovoltaic power interval in hour h and scenario *s*, respectively. The value 1 indicates the selection of corresponding interval. $q_{kl,h}$, $q_{kwt,h}$ and $q_{kpv,h}$ are the probability of *kl*, *kwt* and *kpv* interval in the PDF of the forecasting error of load, wind output power and photovoltaic output power, respectively. $\gamma^{IIDG}_{i,h,s}$ denotes the share of the IIDG outage probability in π_s which can be also determined in a similar way using the applied MCS strategy in a 24 h scheduling time horizon. $W^{IIDG}_{i,h,s}$ is a randomly generated binary variable shows availability status of the *i*th IIDG at hour h and in scenario s, where $W^{IIDG}_{i,h,s} = 1$ means that *i*th IIDG will be available in hour h and scenario s and $W^{IIDG}_{i,h,s} = 0$ expresses that the IIDG *i* is out of service in that hour. FOR^{IIDG}_{i} is employed to explain Forced Outage Rate (FOR) of *i*th IIDG.

The dependency of the computational requirements to the number of generated scenarios makes it necessary to use an effective scenario reduction algorithm for solving the large scale scenario based optimization models. The cornerstone of the scenario reduction algorithms is based on discarding the low probable or very similar scenarios. In this paper, the simultaneous backward scenario reduction technique is applied to satisfy the trade-off between the computational efficiency and the solution accuracy [44]. Concisely, in the proposed scenario reduction algorithm, it is aimed to reduce the number of the generated scenarios such that the scenarios with minimum distance in probability and scenario structure are removed [44,45].

Second stage: MILP-based optimization

In the proposed optimization framework, the microgrid expected frequency excursions should be minimized such that the day-ahead operational cost and emission levels lie in the pre-specified secure ranges. Moreover, the technical constraints of the microgrid energy and reserve management are also taken into account.

Constraints

(1) *Power balance*. Hourly power balance in the islanded microgrid in the normal and during the primary and secondary control levels are denoted in Eqs. (12) and (13) as follows:

$$\sum_{i=1}^{Ng} P_g(i,h) + \sum_{w=1}^{Nw} P_w(w,h) + \sum_{v=1}^{Nv} P_v(v,h) + \sum_{k=1}^{Nk} Pd(k,h) = Load(h) \tag{12}$$

$$\sum_{i=1}^{Ng} P^s_g(i,l,h) + \sum_{w=1}^{Nw} P^s_w(w,l,h) + \sum_{v=1}^{Nv} P^s_v(v,l,h) + \sum_{k=1}^{Nk} Pd^s(k,l,h) = Load^s(l,h) + \Delta P^d(s,l,h) - LSH(s,l,h),\ \forall l = pri,\ sec \tag{13}$$

Worth mentioning that the WT, PV units are not participated in the primary and secondary control levels, therefore, the amount of their generated active power are not changed during the primary and secondary control levels. Likewise, the amount of the accepted energy of the DRPs will not be changed over the primary control level and equals to its accepted energy level in the normal condition as explained by Eq. (15). Besides, it is assumed that the commitment state and the reference power set-points of the available IIDGs are not changed during primary level as described by Eqs. (14)–(17):

$$Pd^s(k,l,h) = Pd(k,h),\ \forall l = pri \tag{14}$$

$$P_{ref}(i,h) = P_g(i,h) \cdot u(i,h) \tag{15}$$

$$W^{IIDG}_{i,h,s} \cdot P^s_{ref}(i,l,h) = W^{IIDG}_{i,h,s} \cdot P^s_g(i,l,h) \cdot u^l(s,i,h),\ \forall l = pri \tag{16}$$

$$W^{IIDG}_{i,h,s} \cdot u(i,h) = W^{IIDG}_{i,h,s} \cdot u^l(s,i,h),\ \forall l = pri \tag{17}$$

It is assumed, whenever the dispatched IIDGs are not capable to generate the required power demands, the EMS is authorized to shed an amount of the microgrid load in the primary and secondary control levels, as expressed by Eqs. (18) and (19):

$$LSH(s,l,h) = Load^s(l,h) - \sum_{i=1}^{Ng} P^s_g(i,l,h) - \sum_{w=1}^{Nw} P^s_w(w,l,h) - \sum_{v=1}^{Nv} P^s_v(v,l,h) - \Delta P^d(s,l,h) - \sum_{k=1}^{Nk} Pd^s(k,l,h),\ \forall l = pri,\ sec \tag{18}$$

$$0 \leqslant LSH(s,l,h) \leqslant Load^s(l,h) \tag{19}$$

Also for the sake of a detailed modeling, the inherent elasticity of the electrical loads to the system frequency is considered as described in Eq. (20):

$$\Delta P^d(s,l,h) = D(s,l,h).\Delta f(s,l,h),\ \forall l = pri,\ sec \tag{20}$$

$\Delta P^d(s,l,h)$ denotes the load contribution due to the load–frequency dependency of the consumers in scenario s and at hour h.

(2) *Frequency dependent constraints of DERs*. To achieve an optimal energy management scheme of a microgrid in accordance to the frequency security aspects, frequency dependent behavior of the droop controlled IIDGs must be modeled precisely. In the primary control level, committed IIDGs should automatically respond to the microgrid frequency excursions according to the droop characteristics and their available power capacity. In the secondary control level, the MGCC is responsible to ensure the microgrid frequency in a robust equilibrium point which can be performed by readjusting the reference power set-points of the available IIDGs. As illustrated in Fig. 2, the available IIDGs and the DRPs, in the primary and secondary control levels, are responsible to alleviate the active power deviations occurred in the microgrid as follows in Eq. (21).

$$\sum_{i=1}^{Ng} W^{IIDG}_{i,h,s} \cdot \Delta P_g(s,i,l,h) = \Delta load(s,l,h) - \sum_{w=1}^{Nw} \Delta P_w(s,w,l,h) - \sum_{v=1}^{Nv} \Delta P_v(s,v,l,h) - \sum_{k=1}^{Nk} \Delta Pd(s,k,l,h) - \sum_{i=1}^{Ng} (1 - W^{IIDG}_{i,h,s}) \cdot \Delta P_g(s,i,l,h) + \Delta P^d(s,l,h) - LSH(s,l,h) \tag{21}$$

Furthermore, in this paper it is assumed that the DRPs are not participated into primary frequency control and sustain their accepted energy levels in the normal condition, therefore, $\sum_{k=1}^{Nk}\Delta Pd(s,k,l,h)\big|_{l=pri}=0$. The MGCC corrective control action applied to each IIDG can be explained by Eq. (22):

$$\sum_{i=1}^{Ng}\Delta P_g(s,i,l,h)=\sum_{i=1}^{Ng}\Delta P_{ref}(s,i,l,h)-\sum_{i=1}^{Ng}\left(\frac{1}{m_p(i)}\right)\cdot\Delta f(s,l,h),\quad \forall l=pri,\ sec \tag{22}$$

Due to Eqs. (15)–(17) and by combining Eqs. (21) and (22), the control functions associated to the LCs and the MGCC can be presented as in Eqs. (23) and (24), respectively:

$$W_{i,h,s}^{IIDG}\cdot u^{l}(s,i,h)\cdot\left(\frac{1}{m_p(i)}\right)\cdot\Delta f(s,l,h)=-W_{i,h,s}^{IIDG}\cdot\Delta P_g(s,i,l,h),\ \ l=pri \tag{23}$$

$$P_g^s(i,l,h)=W_{i,h,s}^{IIDG}\cdot u^{l}(s,i,h)\cdot\left[P_{ref}^s(i,l,h)-\left(\frac{1}{m_p(i)}\right).\Delta f(s,l,h)\right],\quad l=\sec \tag{24}$$

In this paper, since only the islanded mode of the microgrid operation has been considered, it is assumed to provide a more reliable power sharing, the EMS as the owner of all the DERs, is allowed to operate all available droop controlled IIDGs as well as the DRPs in a cost-effectively coordinated framework. Furthermore, to ensure the frequency excursions are controlled in a secure range, it is assumed the microgrid primary and secondary frequency excursions must be smaller than some maximum allowable frequency excursion limits which can be determined by means of the EMS, as follows in Eq. (25).

$$|\Delta f(s,l,h)|\leqslant\Delta f_l^{\max},\ \ \forall l=pri,\ \sec \tag{25}$$

(3) *Techno-economic constraints of DERs.* DERs must satisfy technical limitations, such as upper and lower active power restrictions of the available committed IIDGs and the scheduled reserve limitations. Eqs. (26)–(31) describe the power and reserve restrictions of the IIDGs:

$$P_g^{\min}(i)\cdot W_{i,h,s}^{IIDG}\cdot u(i,h)\leqslant P_g(i,h)\leqslant P_g^{\max}\cdot W_{i,h,s}^{IIDG}u(i,h) \tag{26}$$

$$P_g^{\min}(i)\cdot W_{i,h,s}^{IIDG}\cdot u^{l}(i,h)\leqslant P_g^s(i,l,h)\leqslant P_g^{\max}(i)\cdot W_{i,h,s}^{IIDG}u^{l}(i,h) \tag{27}$$

$$R_g(i,l,ud,h)\geqslant W_{i,h,s}^{IIDG}\cdot(P_g^s(i,l,h)-P_g(i,h)),\ \forall l=pri,\ \forall ud=up \tag{28}$$

$$R_g(i,l,ud,h)\geqslant W_{i,h,s}^{IIDG}\cdot(P_g(i,h)-P_g^s(i,l,h)),\ \forall l=pri,\ \forall ud=dn \tag{29}$$

$$R_g(i,l,ud,h)\geqslant W_{i,h,s}^{IIDG}\cdot(P_{ref}^s(i,l,h)-P_g(i,h)),\ \forall l=sec,\ \forall ud=up \tag{30}$$

$$R_g(i,l,ud,h)\geqslant W_{i,h,s}^{IIDG}\cdot(P_g(i,h)-P_{ref}^s(i,l,h)),\ \forall l=sec,\ \forall ud=dn \tag{31}$$

Eqs. (28)–(31) describe that the precise amounts of the IIDG control reserves are determined in proportion to the largest possible values of the primary frequency excursions among all selected scenarios at each hour. Besides, the DRPs should consider the up/down demand side reserve constraints as follows in Eqs. (32) and (33):

$$R_d(k,l,ud,h)\geqslant(Pd^s(k,l,h)-Pd(k,h)),\ \forall l=sec,\ \forall ud=dn \tag{32}$$

$$R_d(k,l,ud,h)\geqslant(Pd(k,h)-Pd^s(k,l,h)),\ \forall l=sec,\ \forall ud=up \tag{33}$$

Furthermore, the IIDGs ramp up/down constraints are considered in a linearized form as follows in Eqs. (34)–(37):

$$P_g(i,h)-P_g(i,h-1)\leqslant ramp_i^{up}\cdot(1-y(i,h))+ramp_i^{su}\cdot y(i,h) \tag{34}$$

$$P_g(i,h-1)-P_g(i,h)\leqslant ramp_i^{dn}\cdot(1-z(i,h))+ramp_i^{sd}\cdot z(i,h) \tag{35}$$

$$y(i,h)-z(i,h)-u(i,h)+u(i,h-1)=0 \tag{36}$$

$$y(i,h)+z(i,h)-1\leqslant 0 \tag{37}$$

Also minimum up/down time constraints of the available IIDGs are satisfied according to the secure boundaries. Besides, operational costs associated to the scheduled energy and reserves are presented as the linear functions in Eqs. (38) and (39), respectively:

$$C_g^E(i,h)=a_i\cdot u(i,h)+b_i\cdot P_g(i,h)+C_i^{SU}\cdot y(i,h)+C_i^{SD}\cdot z(i,h) \tag{38}$$

$$C_g^R(i,l,ud,h)=\rho_R(i,l,ud)\cdot R_g(i,l,ud,h) \tag{39}$$

Costs of operation of the renewable energy sources including WT and PV units are described by Eq. (40):

$$C_{RES}(h)=\rho_w\cdot\sum_{w=1}^{Nw}P_w(w,h)+\rho_v\cdot\sum_{v=1}^{Nv}P_v(v,h) \tag{40}$$

Eqs. (41) and (42) present the stochastic operational costs of the IIDGs and RESs:

$$C_g^s(i,l,h)=a_i\cdot u^{l}(i,h)+b_i\cdot P_g^s(i,l,h),\ \ \forall l=pri,\ \ sec \tag{41}$$

$$C_{RES}^s(l,h)=\rho_w\cdot\sum_{w=1}^{Nw}P_w^s(w,l,h)+\rho_v\cdot\sum_{v=1}^{Nv}P_v^s(v,l,h),\ \ \forall l=pri,\ \ sec \tag{42}$$

Also, the costs corresponding to the demand response programs can be calculated by Eqs. (43)–(45):

$$C_d^E(k,h)=\sum_{m=1}^{M}\alpha_m(k)\cdot Pd_m(k,h) \tag{43}$$

$$C_d^R(k,l,ud,h)=\rho_d^R(k)\cdot R_d(k,l,ud,h) \tag{44}$$

$$C_d^s(k,l,h)=\sum_{m=1}^{M}\alpha_m(k)\cdot Pd_m^s(k,l,h) \tag{45}$$

The day-ahead microgrid total operational cost including the costs of the energy and reserve provision as well as the costs corresponding to the operational requirements in the reduced scenarios can be described by Eq. (46):

$$Cost_{MG}=\sum_{h=1}^{Nh}\left[\begin{array}{l}\left(\begin{array}{l}\sum_{i=1}^{Ng}C_g^E(i,h)+\sum_{i=1}^{Ng}\sum_{l}\sum_{ud}C_g^R(i,l,ud,h)\\ +C_{RES}(h)+\sum_{k=1}^{Nk}C_d^E(k,h)+\sum_{k=1}^{Nk}\sum_{l=sec}\sum_{ud}C_d^R(k,l,ud,h)\end{array}\right)\\ +\sum_{s=1}^{Ns}\pi_s\cdot\left(\sum_{l}\left(\sum_{i=1}^{Ng}C_g^s(i,l,h)+C_{RES}^s(l,h)+\sum_{k=1}^{Nk}C_d^s(k,l,h)\right)\right)\\ +VOLL.ELNS(h)\end{array}\right] \tag{46}$$

The term ELNS stands for the expected load not served and can be expressed by Eq. (47).

$$ELNS(h)=\sum_{s=1}^{Ns}\pi_s\cdot\sum_{l}[LSH(s,l,h)] \tag{47}$$

VOLL represents the value of lost load which has been determined by means of the EMS. To consider the environmental purposes of the microgrid operational planning, total day-ahead produced CO_2 emission of the dispatchable IIDGs can be formulated as Eq. (48):

$$Emission_{MG} = \sum_{h=1}^{Nh}\left[\sum_{i=1}^{Ng}\Omega_i^{CO_2}\cdot P_g(i,h) + \sum_{s=1}^{Ns}\pi_s\cdot\left(\sum_{i=1}^{Ng}\sum_{l}\Omega_i^{CO_2}\cdot P_g^s(i,l,h)\right)\right] \quad (48)$$

Objective function

In this paper, it is assumed, the microgrid frequency will be controlled as the main objective function. Eq. (49) explains the mathematical modeling of the proposed objective function:

$$Frequency_{MG} = \sum_{s=1}^{Ns}\pi_s\cdot\left(\sum_{h=1}^{Nh}\sum_{l}|\Delta f(s,l,h)|\right) \quad (49)$$

It is aimed to manage the islanded microgrid frequency subject to the reasonable operational cost and emission requirements and in accordance to the EMS operational policies. Succinctly, the proposed optimization framework can be presented as follows in Eq. (50):

$$\begin{aligned} &Min\ Frequency_{MG}\\ &s.t.\\ &Cost_{MG} \leqslant \eta_{MG}^{C}\\ &Emission_{MG} \leqslant \eta_{MG}^{E} \end{aligned} \quad (50)$$

where η_{MG}^{C} and η_{MG}^{E} are allowable microgrid cost and emission operational levels through which the frequency management approach is justified.

As it can be observable in the objective function description, there is an absolute function which causes the model to appear as a non-linear model. To make this nonlinear term behave linearly, two positive variable as $\Delta f^{+}(s,l,h)$ and $\Delta f^{-}(s,l,h)$ are defined and convert the nonlinear function ($|\Delta f(s,l,h)|$) to a linear term as described in Eq. (51):

$$\begin{aligned} &|\Delta f(s,l,h)| = \Delta f^{+}(s,l,h) + \Delta f^{-}(s,l,h);\\ &\Delta f(s,l,h) = \Delta f^{+}(s,l,h) - \Delta f^{-}(s,l,h); \end{aligned} \quad (51)$$

By substitution of the linearized Eq. (51) into the proposed MILP model, the microgrid energy management system has this capability to consider either positive and negative frequency excursions. For example, if the net power deviation causes the positive frequency excursion, the amount of $\Delta f^{-}(s,l,h)$ will be zero and $\Delta f(s,l,h) = \Delta f^{-}(s,l,h)$. Vice-versa $\Delta f^{+}(s,l,h)$ becomes zero in the scenarios net power deviations cause negative frequency excursions.

Simulation and numerical results

The considered microgrid test system is depicted in Fig. 7. It is assumed all the IIDGs including two Fuel Cells (FCs), two Micro-Turbines (MTs) and a Gas Engine (GE) are controlled using the proposed *P–f* droop method. Three wind turbines with total 250 kW and two photovoltaic panels with total 140 kW capacities are also considered. The operational costs corresponding to the WTs and PVs active power output are 10.63 and 54.84 cents/kW h, respectively [16]. In this study, the FOR of all the IIDGs are assumed to be equal to 0.03. Technical and economical data of the simulated microgrid have been taken from [16] and listed in Tables 1 and 2, respectively.

Two DRPs using step-wise price-demand packages are considered to be participated into the proposed energy management system. Table 3 illustrates the DRPs' offer packages.

The forecasted values of the microgrid hourly load, WT and PV active power generations are depicted in Fig. 8.

The value of lost load (VOLL) has been selected as 1000 cent/kW h. In the first stage of optimization, 20 reduced scenarios have been remained and applied to the second MILP based optimization stage to minimize the expected frequency excursion over a 24 h time horizon. In the second stage, two case-studies have been defined as illustrated by Table 4. In case 1 the DR programs are

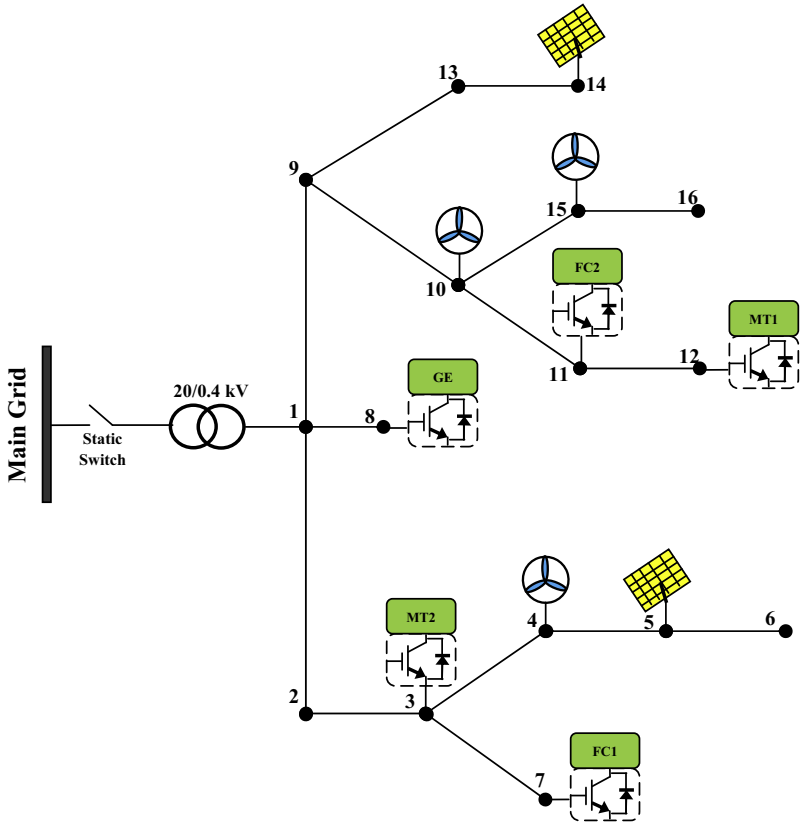

Fig. 7. Microgrid test system.

Table 1
The technical data of microgrid dispatchable IIDGs.

DG unit	P_g^{min} (kW)	P_g^{max} (kW)	$ramp^{up/dn}$ (kW)	$ramp^{su/sd}$ (kW)	m_p (MHz/kW)	Ω^{CO_2} (kg/kW h)
MT	25	150	100	150	10.00	0.550
FC	20	100	100	100	15.00	0.377
GE	35	200	150	200	7.50	0.890

Table 2
The economic data of microgrid dispatchable IIDGs.

DG unit	a_i (cents/h)	b_i (cents/kW h)	C_i^{SU} (cents)	C_i^{SD} (cents)	$\rho_i^{up/dn}(l = pri)$ (cents/kW h)	$\rho_i^{up/dn}(l = sec)$ (cents/kW h)
MT	85.06	4.37	9	8	6.00	2.10
FC	255.18	2.84	16	9	4.00	1.50
GE	212.00	3.12	12	8	3.80	1.70

Table 3
Price-demand offered package of the DRPs.

DRP1	Demand (kW)	0–25	25–65	65–95	95–120
	Offered price (cents)	0.3	0.48	0.60	0.75
DRP2	Demand (kW)	0–40	40–60	60–85	85–135
	Offered price (cents)	0.25	0.45	0.65	0.80

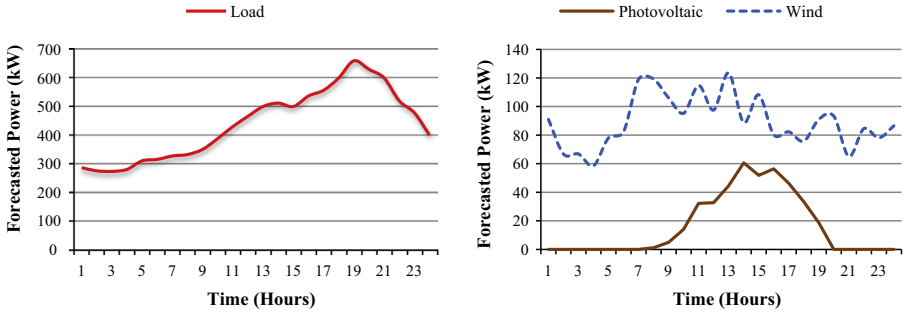

Fig. 8. Forecasted active power values of Load, WT and PV units.

Table 4
The considered case-studies by means of EMS.

Case	η^C_{max} (cent)	η^E_{max} (kg)	Δf^{max}_{pri} (MHz)
Case 1	400,000	14,750	±350
Case 2	225,000	8200	±350

not included in the EMS, while case 2 presents an energy management system in which the proposed ancillary service DR programs are integrated. It has been considered in both cases the MGCC manages the available reserve resources such that the secondary frequency will be restored to its nominal value.

Worth to be mentioned, the EMS may be able to control the microgrid frequency excursions as minimum as possible, however, the values of the associated operational cost and emission will become very expensive which does not match to the microgrid eventual goals. To verify this claim, two simple payoff tables have been drawn out in $\varphi 1$ and $\varphi 2$ matrices. Thus, owing to the superior importance of the microgrid security procurement, particularly in islanded mode, the present paper proposes a highly constraint optimization problem in order to manage the microgrid frequency in a cost-effective manner. To attain an appropriate solution, the MILP model is solved using the powerful CPLEX solver in the GAMS environment [46]. The values of η^C_{max} and η^E_{max} can be easily obtained using a simple analysis over the calculated payoff tables as well as in accordance to the EMS decision makings. In the $\varphi 1$

Table 5
Break-down of the optimization results.

Case	$Cost_{MG}$ (cent)	$Emission_{MG}$ (kg)	$Frequency_{MG}$ (MHz)	$ELNS$ (kW h)	Energy providing cost			Reserve scheduling cost		
					IIDG	RES	DR	Primary	Secondary	DR
1	395170.67	14701.78	0.241	128.60	50543.18	46399.93	–	13851.75	4937.37	–
2	217128.38	8171.14	0.289	0.398	32033.57	46399.93	1079.99	15380.49	3942.45	544.21

and $\varphi 2$, the left, middle and right columns are maximum and minimum values of $Cost_{MG}$, $Emission_{MG}$ and $Frequency_{MG}$, respectively.

$$\varphi 1|_{case1} = \begin{bmatrix} 375188.239 & 16714.547 & 3.154 \\ 7851854.191 & 8125.720 & 4.642 \\ 5703339.711 & 12581.613 & 0.461 \end{bmatrix};$$

$$\varphi 2|_{case2} = \begin{bmatrix} 190958.979 & 8217.742 & 4.906 \\ 10691446.366 & 1842.245 & 6.212 \\ 7727403.846 & 8178.501 & 0.487 \end{bmatrix}$$

The optimization results over the considered 24 h time horizon have been broken down in Table 5.

Comparing the optimization results in cases 1 and 2 reveals that employing the DR programs reduces the amounts of the microgrid day-ahead operational cost and emission levels. Besides, the amount of the involuntary load shedding in case 2 has been significantly decreased as it is understandable from the ELNS values in Table 5. The striking outcome from the incorporation of the DR programs into the microgrid frequency management procedure can be interpreted by the reduced cost associated to the provided energy by the IIDGs within18059.61 cent Day^{-1}. Furthermore, the DR integration causes the cost of the scheduled secondary control reserves to be decreased from 4937.37 to 3942.45 cents. However, the cost of the primary control reserves has been increased in case 2. It is because of that the DR programs have not been participated in the primary frequency control level. On the other hand, the participation of the DRPs into the providing the energy requirements of the microgrid resulted to that the expensive IIDGs do not commit in some hours. This makes the primary frequency excursions be larger due to the lower amounts of the online droop controllers. The greater amount of $Frequency_{MG}$ in case 2 verifies this claim. As a result, the remained committed IIDGs have to generate more active power in the primary level to cope with the greater primary frequency excursion. Hence, the scheduled primary reserves in case 2 have became more costly comparing to case 1. Nevertheless, total operational costs have been considerably reduced and DR programs economized microgrid hierarchical frequency control.

Figs. 9 and 10 show the provided energy in cases 1 and 2, respectively. Clearly, in case 2 where the DR programs have been employed, the provided energy by the IIDGs is reduced and accordingly the total operational cost and emission have been decreased.

The amounts of the scheduled up/down primary control reserves in cases 1 and 2 are depicted in Figs. 11 and 12, respectively. Negative values indicating the downward frequency control reserves.

Generally, the amounts of the scheduled primary control reserves depends to the maximum amount of the positive or negative hourly primary frequency excursions among all the reduced scenarios, number of the committed units of each IIDG type and the *P–f* droop characteristics of available committed IIDGs. For example, in case 1, at hour 15, the maximum negative and positive primary frequency excursions are −291.545 and +116.091 MHz,

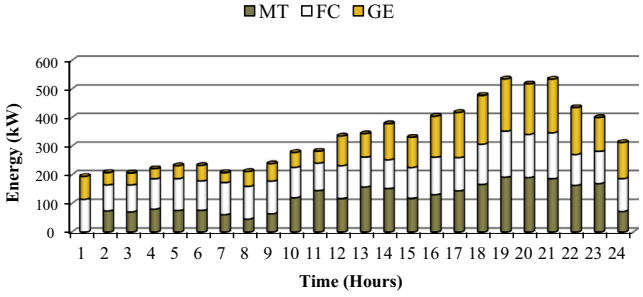

Fig. 9. Provided energy in case 1 without DR.

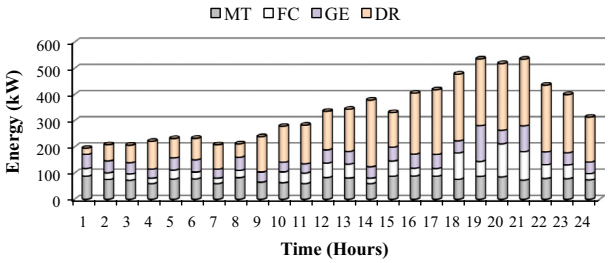

Fig. 10. Provided energy in case 2 with DR.

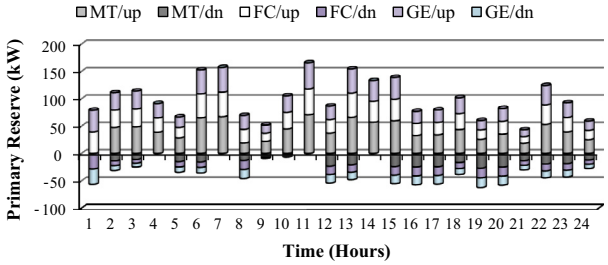

Fig. 11. Up and down primary frequency control reserves of available IIDGs in case 1.

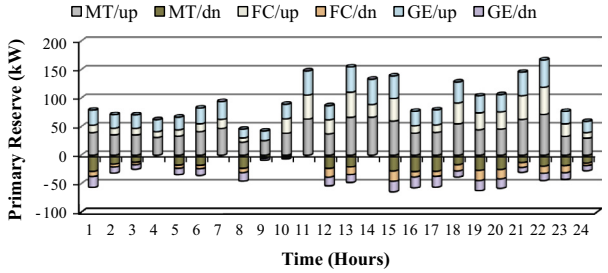

Fig. 12. Up and down primary frequency control reserves of available IIDGs in case 2.

respectively and all the IIDGs have been committed. Therefore, the precise amounts of scheduled upward primary reserves are 29.779 kW for each MT, 19.825 kW for each FC and 39.705 kW for GE. Likewise, scheduled downward primary reserves are 11.806 kW for each MT, 7.870 kW for each FC, and 15.741 kW for GE. In case 2, at hour 24, because of the presence of DRPs in the microgrid energy and reserve scheduling, one of the FC units has not been committed and the other unit has generated 24.54 kW which is also close to its minimum value. As a result, participation of the FC units in the primary frequency control reserves has been halved in comparison to the condition in which two FCs have been committed. Generally, as discussed above, the amounts of the primary frequency control reserves are larger in case 2, where DR programs are considered with respect to case 1, because lower number of the committed IIDGs yields greater frequency excursions and accordingly requires higher primary reserves.

Figs. 13 and 14 demonstrate the scheduled up/down secondary frequency control reserves in cases 1 and 2, respectively. Typically, secondary control reserves are managed by means of the MGCC such a way the microgrid cost and emission secure ranges will be satisfied. The MGCC changes the reference power set-points of the IIDGs to determine the amounts of adequate secondary control reserves and restore the frequency excursions of each scenario to the nominal value.

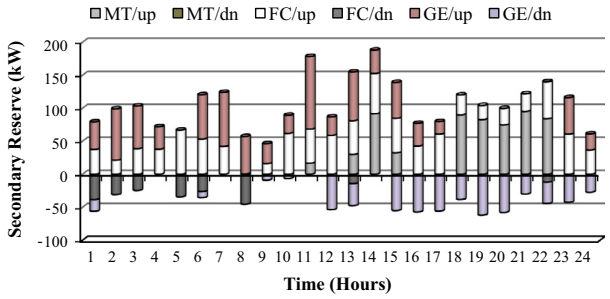

Fig. 13. Up and down secondary frequency control reserves in case 1.

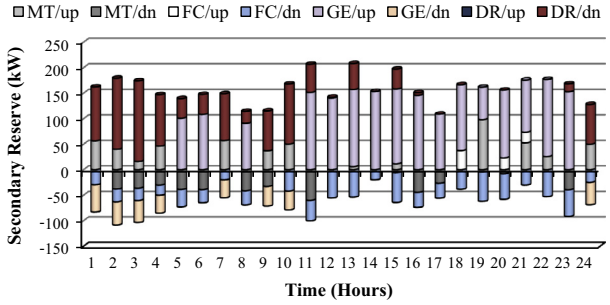

Fig. 14. Up and down secondary frequency control reserves in case 2.

Observably, the participation of the demand response programs into the secondary control level reduces the cost of the scheduled secondary control reserves from 4937.37 to 4486.66 cents Day^{-1}. For a more detailed analysis, the optimization results during the scenario 5 with the highest probability have been broken down over three hours. The selected hours are 2, 11 and 19 with 275, 430 and 660 kW forecasted load demands, respectively. The hours have been chosen such that all the off-peak, valley and peak load consumptions have been analyzed. The techno-economic optimization results and the associated expected values in the scenario 5 are listed in Table 6. Furthermore, the provided energy and active power outputs of the IIDGs related to the LCs and the MGCC frequency control functions in the primary and secondary levels are represented in Table 7.

In hour 2, the microgrid experiences 38.98 kW total active power deviation which consists 16.20 kW WT and 55 kW load consumption rises. The committed IIDGs and accepted DRPs are in charge to compensate the 38.98 kW power shortage that causes the microgrid frequency to fall within 82.555 MHz in case 1 and 96.314 MHz in case 2. These frequency excursions can be easily calculated according to Eq. (23) as follows:

$$\Delta f(5,pri,2)|_{case1} = \frac{-38.980+0.453}{1/0.01+1/0.01+1/0.015+1/0.015+1/0.0075} = -0.082557\,\text{Hz}$$

$$\Delta f(5,pri,2)|_{case2} = \frac{-38.980+0.528}{1/0.01+1/0.01+1/0.015+1/0.015.(0)+1/0.0075} = -0.096131\,\text{Hz}$$

In case 2, one of the IIDGs have not been committed and the primary frequency excursion fallen more severely. The LCs must increase the committed IIDGs active power outputs corresponding to the IIDG *P–f* droop characteristics as presented in Table 7. For example, in hour 2, in case 1, two committed FCs have released $2 \times 0.082557/0.015 = 11.007$ kW primary active power output to compensate the primary frequency drop. However, in case 2, one of the FC units has not been committed and the released primary active power has been decreased.

Analogously, in hour 19, the EMS must cope with 21.84 kW wind power increase, 7.14 kW photovoltaic power output increase and 33 kW load consumption decrease and consequently totally 61.98 kW active power surplus. Accordingly, the primary frequency excursion rises within +129.905 MHz according to Eq. (24). The committed IIDGs in this condition must decrease their active power output to mitigate the risen primary frequency excursion owing to Table 7. For example, in case 1, the GE unit reduces its active power output from 182.771 to 165.063 kW. The MGCC readjusts the reference power set-points of the available IIDGs to restore the microgrid frequency to its nominal value. The MGCC should also consider the economic-environmental policies of the energy management system according to Table 7.

Noticeably, modeling the load–frequency dependency in the primary frequency control makes the frequency excursions be lighter and help committed IIDGs generating lower primary active power and therefore reducing the hourly operation cost and emission. For example, in case 2, in hour 2, the frequency excursion would occur on 0.097450 Hz if the load contribution neglected. This would cause the committed IIDGs to generate 185.528 kW comparing to 185 kW in which the load–frequency dependency has been modeled. Besides, integration of the DR programs in case 2 has an efficient effect on decreasing the total cost and emission levels with. Also, the amounts of the active power outputs of the IIDGs in both the primary and secondary control levels have been reduced in case 2. Meanwhile, the MGCC and the LCs have provided control functions with higher degrees of freedom due to the active participation of the demand side resources in the microgrid energy and reserve scheduling.

To provide a more robust energy management system, possibility of the DER outages due to the occurrence of a random contingency is also taken into account in the scenario generation procedure. By this way, the EMS has to control the frequency excursions not only with the consideration of the RES

Table 6
Techno-economic optimization results in scenario 5 over considered hours 2, 11 and 19.

Hour	Case	Total active power variation (kW)	Primary frequency excursion (MHz)	Primary load contribution (kW)	Total generation level of IIDGs (kW)		Total emitted CO_2 (kg)		Total generation cost (cents)	
					Primary	Secondary	Primary	Secondary	Primary	Secondary
Hour 2	1	38.980	−82.557	−0.453	247.230	247.230	136.99	137.60	1756.01	1753.12
	2	38.980	−96.131	−0.528	185.000	45.715	116.10	25.14	1324.38	284.83
Hour 11	1	51.560	−108.486	−0.933	334.515	334.610	184.28	172.90	2000.74	1973.67
	2	51.560	−108.486	−0.933	186.560	131.56	110.04	117.08	1561.84	622.46
Hour 19	1	61.980	129.905	1.357	473.838	473.700	291.80	273.68	2723.12	2796.37
	2	61.980	129.905	1.357	218.700	218.700	153.72	166.66	1638.62	1167.33

Table 7
Generation levels related to the LCs and MGCC in scenario 5 at hours 2, 11 and 19.

DER	Case	EMS provided energy (kW)			LC active power output (kW)			MGCC reference power set-point (kW)		
		Hour 2	Hour 11	Hour 19	Hour 2	Hour 11	Hour 19	Hour 2	Hour 11	Hour 19
MTs	1	73.294	144.355	191.537	90.000	166.451	164.974	73.294	144.355	191.536
	2	75.510	60.000	86.562	95.000	82.096	60.000	45.715	–	82.291
FCs	1	91.092	96.236	161.370	102.230	110.967	143.662	112.112	147.796	161.370
	2	25.170	40.000	57.708	31.666	54.730	40.000	–	–	–
GE	1	43.862	42.458	182.771	55.000	57.189	165.063	61.822	42.458	120.791
	2	45.328	35.000	80.160	58.304	49.704	62.491	45.328	35.000	52.807
DRs	1	–	–	–	–	–	–	–	–	–
	2	62.230	148.050	255.000	62.230	148.050	255.000	201.515	203.050	255.000

Table 8
The optimization results in contingency scenario at hour 22 in cases 1 and 2.

Case	Primary frequency excursion (MHz)	DG	Provided energy (kW)	Scheduled up-reserve (kW)		Generation level (kW)	
				Primary	Secondary	Primary	Secondary
1	−260.508	MTs	162.865	53.262	83.88	205	246.736
		FC1	82.245	17.754	0	100	82.245
		FC2	26.325	17.754	55.92	0	0
		GE	164.071	35.508	0.42	200	164.491
2	−350.000	MTs	78.976	71.56	0	150.536	104.779
		FC1	26.325	28.853	49.053	50.179	0
		FC2	26.325	28.853	0	0	0
		GE	48.871	47.706	101.540	96.578	200
		DRs	255.000	–	–	255.000	255.000

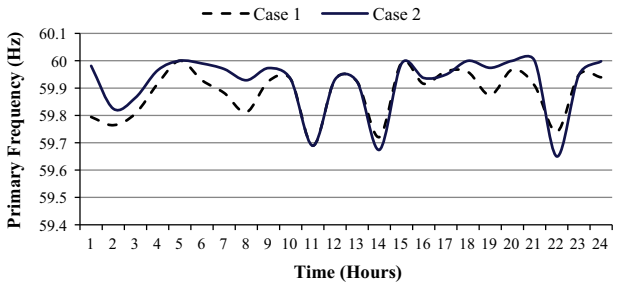

Fig. 15. RMS-primary frequency profile in scenario 12 over the 24 h.

intermittency and load fluctuations, but also subject to the possible contingencies associated to the committed IIDGs. In scenario 12, a contingency occurred and the FC2 unit has been out of the service in hour 22. The optimization results are listed in Table 8. As it is presented, in case 2, the primary frequency excursion has been set at −350 MHz which is the maximum allowable frequency excursion limit. In other words, total active power deviation in this case has been 150.606 kW power deficits. This power variation causes the microgrid primary frequency excursion to fall within 376.515 MHz which is beyond the allowable frequency range. Therefore, the EMS has to unwillingly shed an amount of microgrid load to set the frequency excursion at maximum allowable margin, i.e. 350 MHz. The amount of load shed can be calculated using Eq. (18) as follows:

$$\begin{aligned} LSH(12,pri,22) &= Load^{12}(pri,22) - \sum_i P_g^{12}(i,pri,22) \\ &\quad - \sum_w P_w(w,pri,22) - \sum_v P_v(v,pri,22) \\ &\quad - \Delta P^d(12,pri,22) - \sum_k Pd^{12}(k,pri,22) \\ &= 624 - 297.29 - 64.22 - 0 - 0.364 - 255 \\ &= 7.48 \text{ kW} \end{aligned}$$

Thus, during the outage of the FC2, the other IIDGs and DRPs have supplied end-user consumption demand and provide robust energy and reserve management framework as illustrated in Table 8. The Root Mean Square (RMS) values of the hourly primary frequency profile in the scenario 12, in which the contingency is occurred, is depicted in Fig. 15. Due to the deactivation of the DR programs in the primary control level, the frequency excursions and consequently microgrid reserve requirements are larger in case 2 at hour 22.

Conclusions

Microgrid frequency is a key control variable which should be managed subject to the EMS operational policies to ensure the microgrid security margins with justified cost and emission levels. The present paper dealt with the cost-effective frequency management of an islanded microgrid. For this purpose, the frequency-dependent of droop controlled IIDGs was modeled precisely in the steady-state. The hierarchical frequency control levels were clearly described and the corresponding mathematical models were formulated using an efficient mixed integer linear programming. Moreover, a demand response program was proposed using a step-wise price-demand package to be participated in the frequency management approach. The MCS strategy was employed to generate some random scenarios which model the forecasting errors related to the intermittency of WT/PV power generations as well as the fluctuations corresponding to the load consumption. Besides, $N-1$ contingency analysis including the possible outages of the IIDGs was implemented to verify the robustness of the proposed frequency aware EMS. Day-ahead numerical results demonstrate the efficiency of the proposed EMS to cost-effectively managing the microgrid frequency. The performances of LCs and the MGCC have been evaluated and the associated primary and secondary control reserves scheduled such that microgrid frequency, cost and emission were sustained into some pre-specified secure ranges. Demand response program integration in the

proposed EMS promoted the microgrid operational aspects in either the system security enhancement or economizing the microgrid operational cost and emission. Lastly, the proposed EMS verifies that the energy management issues in microgrids should be scheduled such that not only ensures the economical targets but also enhances the frequency security margins by precisely modeling the microgrid frequency dependent control functions.

References

[1] Katiraei F, Iravani R, Hatziargyriou N, Dimeas A. Microgrids management. IEEE Power Energy Mag 2008;6(3):54–65.
[2] Lasseter RH, Paigi P. Microgrid: a conceptual solution. In: Proceeding of 35th annual IEEE power electronics specialists conference; 2004. p. 4285–90.
[3] Hatziargyriou N, Asano H, Iravani R, Marnary C. Microgrids. IEEE Power Energy Mag 2007;5(4):78–94.
[4] Jimeno J, Anduaga J, Oyarzabal J, de Muro AG. Architecture of a microgrid energy management system. Eur Trans Electr Eng 2011;21:1142–58.
[5] Vandoorn TL, Vasquez JC, Kooning JD, Guerrero JM, Vandevelde L. Microgrids: hierarchical control and on overview of the control and reserve management strategies. IEEE Ind Electron Mag 2013:42–55.
[6] Guerrero JM, Chandorkar M, Lee TL, Loh PC. Advanced control architecture for intelligent microgrids – Part I: Decentralized and hierarchical control. IEEE Trans Ind Electron 2013;60(4):1254–62.
[7] Guerrero JM, Vasquez JC, Matas J, de Vicuna LG, Castilla M. Hierarchical control of droop-controlled AC and DC microgrids – a general approach toward standardization. IEEE Trans Ind Electron 2011;58(1):387–405.
[8] Justo JJ, Mwasillu F, Lee J, Jung JW. AC-microgrids versus DC-microgrids with distributed energy resources: a review. Renew Sustain Energy Rev 2013;24:387–405.
[9] Palizban O, Kauhaniemi K, Guerrero JM. Microgrids in active network management – Part I: Hierarchical control, energy storage, virtual power plants, and market participation. Renew Sustain Energy Rev 2014. Early access.
[10] Rocabert J, Luna A, Blaabjerg F, Rudriguez P. Control of power converters in AC microgrids. IEEE Trans Power Electron 2012;27(11):4734–49.
[11] Lopez JAP, Moreira CL, Madureira AG. Defining control strategies for microgrids islanded operation. IEEE Trans Power Syst 2006;21(2):916–24.
[12] Bidram A, Davoudi A. Hierarchical structure of microgrids control system. IEEE Trans Smart Grid 2012;3(4):1963–76.
[13] Olivares DE, Canizares CA, Kazerani M. A centralized optimal energy management system for microgrids. In: IEEE PES general meeting; 2011. p. 1–6.
[14] Planas E, de Muro AG, Andreu J, Kortabarria I, de Alegria IM. General aspects, hierarchical controls and droop methods in microgrids: a review. Renew Sustain Energy Rev 2013;17:147–59.
[15] Eid BL, Rahim NA, Selvaraj J, Al Khateb AH. Control methods and objectives for electronically coupled distributed energy resources in microgrids: a review. IEEE Syst J 2014. Early access.
[16] Tsikalakis AG, Hatziargyriou ND. Centralized control for optimizing microgrids operation. IEEE Trans Energy Convers 2008;23(1):241–8.
[17] Galiana FD, Bouffard F, Arroyo JM, Restrepo JF. Scheduling and pricing of coupled energy and primary, secondary and tertiary reserves. Proc IEEE 2005;93(11):1970–83.
[18] Wood AJ, Wollenberg BF. Power generation, operation and control. New York: Willey; 1984.
[19] Rabbanifar P, Jadid S. Stochastic multi-objective security-constrained market clearing considering static frequency of power system. Int J Electr Power Energy Syst 2014;54:465–80.
[20] US department of Energy. Benefits of demand response in electricity markets and recommendations for achieving them. Report to US congress. <http://eetd.lbl.gov/EA/EMS/reports/congress-1252d.pdf>; 2006.
[21] Faria P, Vale Z. Demand response in electrical energy supply: an optimal real time pricing approach. Energy 2011;36:5374–84.
[22] Liu G, Tomsovic K. A full demand response model in co-optimized energy and reserve markets. Electr Power Syst Res 2014;111:62–70.
[23] Wu H, Shahidehpour M, Al-Abdulwahab A. Hourly demand response in day-ahead scheduling for managing the variability of renewable energy. IET Gener, Transm Distrib 2013;7(3):226–34.
[24] Sahin C, Shahidehpour M, Erkmen I. Allocation of hourly reserve versus demand response for security-constrained scheduling of stochastic wind energy. IEEE Trans Sustain Energy 2013;4(1):219–28.
[25] Falsafi H, Zakariazadeh A, Jadid S. The role of demand response in single and multi-objective wind-thermal generation scheduling: a stochastic programming. Energy 2014;64:853–67.
[26] Zakariazadeh A, Jadid S, Siano P. Economic-environmental energy and reserve scheduling of smart distribution systems: a multi-objective mathematical programming approach. Energy Convers Manage 2014;78:151–64.
[27] Moghaddam AA, Seifi A, Niknam T, Alizadeh Pahlavani MR. Multi-objective operation management of a renewable microgrid with back-up micro-turbine/fuel cell/battery hybrid power source. Energy 2011;36:6490–507.
[28] Chen C, Duan S, Cai T, Liu B, Hu G. Smart energy management strategy for optimal microgrid economic operation. IET Renew Power Gener 2011;5(3):258–67.
[29] Motavasel M, Seifi AR. Expert energy management of a microgrid considering wind energy uncertainty. Energy Convers Manage 2014;83:58–72.
[30] Mohammadi S, Soleymani S, Mozafari B. Scenario-based stochastic operation management of microgrid including wind, photovoltaic, micro-turbine, fuel cell and energy storage devices. Int J Electr Power Energy Syst 2014;54:525–35.
[31] Marzband M, Sumper A, Ruiz-Alvarez A, Garcia JLD, Tomoiuga B. Experimental evaluation of a real time energy management system for stand-alone microgrids in day-ahead markets. Appl Energy 2013;106:365–76.
[32] Marzband M, Ghadimi M, Sumper A, Garcia JLD. Experimental validation of a real-time energy management system using multi-period gravitational search algorithm for microgrids in islanded mode. Appl Energy 2014;128:164–74.
[33] Zakariazadeh A, Jadid S, Siano P. Stochastic multi-objective operational planning of smart distribution systems considering demand response programs. Electr Power Syst Res 2014;111:156–68.
[34] Zakariazadeh A, Jadid S, Siano P. Stochastic operational scheduling of smart distribution systems considering wind generation and demand response programs. Int J Electr Power Energy Syst 2014;63:218–25.
[35] Barklund E, Pogaku N, Prodanovic M, Hernandez-Aramburo E, Green TC. Energy management in autonomous microgrid using stability constraint droop control of inverters. IEEE Trans Power Electron 2008;23(5):2346–52.
[36] Hernandez-Aramburo CA, Green TC, Mugniot N. Fuel consumption minimization of a microgrid. IEEE Trans Ind Appl 2005;41(3):673–81.
[37] Divshali PH, Hosseinian SH, Abedi M. A novel multi-stage fuel cost minimization in a VSC-based microgrid considering stability, frequency and voltage constraints. IEEE Trans Power Syst 2013;28(2):931–9.
[38] Conti S, Nicolosi R, Rizzo SA, Zeineldin HH. Optimal dispatching of distributed generators and storage systems for MV islanded microgrids. IEEE Trans Power Deliv 2012;27(3):1243–51.
[39] Rezaei N, Kalantar M. Economic–environmental hierarchical frequency management of a droop-controlled islanded microgrid. Energy Convers Manage 2014;88:498–515.
[40] Mahmoud MS, Hussian SA, Abido MA. Modeling and control of microgrid: an overview. J Franklin Inst 2014;351(5):2822–59.
[41] Michalewicz Z. Genetic algorithm + data structure = evaluation program. New York (USA): Springer-Verlag; 1996.
[42] Billinton R, Allan RN. Reliability evaluation of power systems. New York (USA): Plenum; 1996.
[43] Aghaei J, Karami M, Muttaqi KM, Shayanfar HA, Ahmadi A. MIP-based stochastic security-constrained daily hydrothermal generation scheduling. IEEE Syst J 2014. Early access.
[44] Wu L, Shahidehpour M, Li T. Stochastic security-constraint unit commitment. IEEE Trans Power Syst 2007;22:800–11.
[45] Aghaei J, Niknam T, Azizipanah-Abaeghooee R, Arroyo JM. Scenario-based dynamic economic emission dispatch considering load and wind power dispatch. Int J Electr Power Energy Syst 2013;47:351–67.
[46] Generalized Algebraic Modeling Systems (GAMS). <http://www.GAMS.com>.